Quantitative Assessment of Agricultural Runoff and Soil Erosion Using Mathematical Modeling: Applications in the Mediterranean Region

G. ARHONDITSIS[*,1]
Department of Marine Sciences
University of the Aegean
81100 Mytilene, Greece

C. GIOURGA
A. LOUMOU
M. KOULOURI
Department of Environmental Studies
University of the Aegean
81100 Mytilene, Greece

ABSTRACT / Three mathematical models, the runoff curve number equation, the universal soil loss equation, and the mass response functions, were evaluated for predicting nonpoint source nutrient loading from agricultural watersheds of the Mediterranean region. These methodologies were applied to a catchment, the gulf of Gera Basin, that is a typical terrestrial ecosystem of the islands of the Aegean archipelago. The calibration of the model parameters was based on data from experimental plots from which edge-of-field losses of sediment, water runoff, and nutrients were measured. Special emphasis was given to the transport of dissolved and solid-phase nutrients from their sources in the farmers' fields to the outlet of the watershed in order to estimate respective attenuation rates. It was found that nonpoint nutrient loading due to surface losses was high during winter, the contribution being between 50% and 80% of the total annual nutrient losses from the terrestrial ecosystem. The good fit between simulated and experimental data supports the view that these modeling procedures should be considered as reliable and effective methodological tools in Mediterranean areas for evaluating potential control measures, such as management practices for soil and water conservation and changes in land uses, aimed at diminishing soil loss and nutrient delivery to surface waters. Furthermore, the modifications of the general mathematical formulations and the experimental values of the model parameters provided by the study can be used in further application of these methodologies in watersheds with similar characteristics.

One of the problems frequently involved in coastal management is that of distinguishing between point and nonpoint discharges, which is essential for effective protection of seawater quality (Paerl 1997). Point sources enter the pollution transport routes at discrete, identifiable locations and usually can be measured directly. On the other hand, nonpoint sources enter surface waters in a diffuse manner and at intermittent intervals that are related mostly to the occurrence of meteorological events. They cannot be monitored at their point of origin and their exact source is difficult or impossible to trace. Therefore, nonpoint sources are inherently difficult to measure and they cannot be assessed in terms of effluent limitations (Novotny and Chesters 1981, Marchetti and Verna 1992).

The difficulties and inaccuracies concerning the prediction of soil loss and direct runoff from various soil and crop combinations encountered in watersheds and the retention and transport processes of nutrients through these systems were partially surpassed by the use of mathematical models (Deaton and Winebrake 1999). Individual components of basins have been modeled with varying levels of success to attempt to understand the interdisciplinary nature of processes operating at the watershed level (Borah 1989, Huber and others 2000). These models can be classified according to their level of sophistication and potential field of application, and each class is efficient for a range of simulations, which, in principle, cover any level of detail the user might deem necessary (Bouraoui and Dillaha 1996).

During the last decade, comprehensive-modeling constructions, focused on deterministic, stochastic, linear or nonlinear interpretations of the coastal systems' behavior have reached an advanced level in North America and Europe (Nikolaidis and others 1998, Bas-

[1]Present address: Department of Civil and Environmental Engineering, University of Washington, 313B More Hall, Box 352700, Seattle, Washington, USA

*Author to whom correspondence should be addressed; *email:* garh@env.aegean.gr
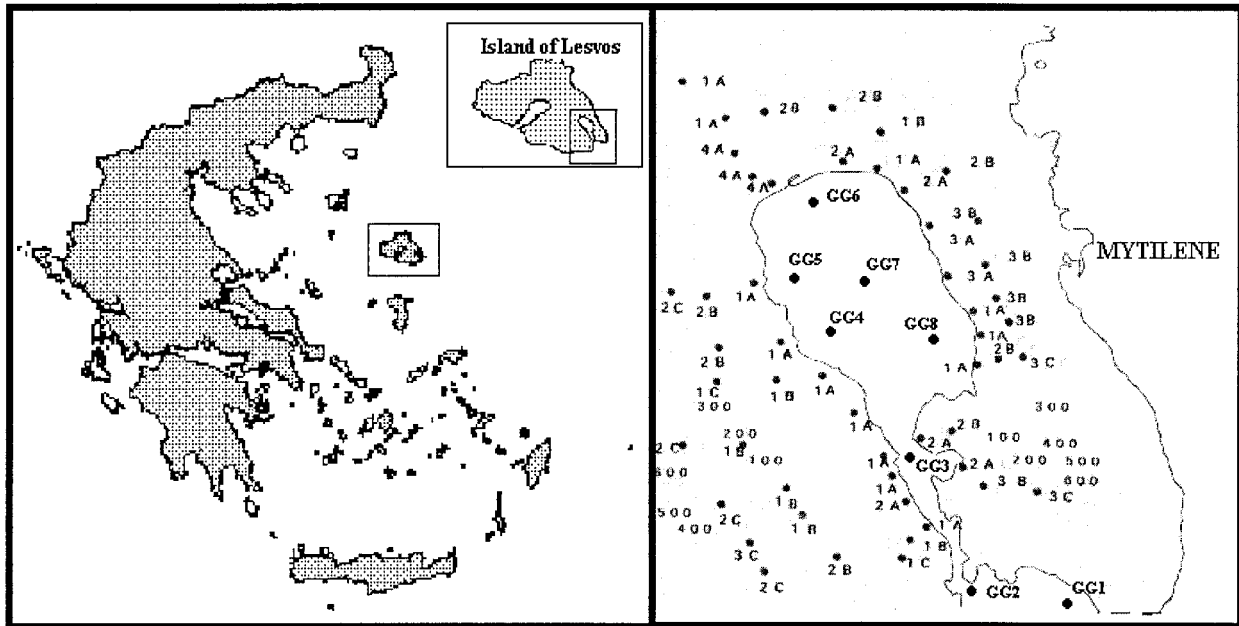
Figure 1. Gulf of Gera, Island of Lesvos, Greece showing the sampling sites of the marine (GG1-GG8) and terrestrial ecosystems. Numbers 1, 2, 3, and 4 correspond to the land cover categories: cultivated olive groves, abandoned olive groves, maquis, and wetlands, respectively. Letters A, B, and C correspond to altitudes of <150, $150–300$, and >300 m, respectively.

nyat and others 1999, Ekholm and others 1999). Meanwhile, similar approaches in the Mediterranean region are still in an early phase and considerable gaps in the literature exist with regard to the computation of regionalized relationships and the objective calibration of the various parameters of well-known algorithms (Bagarello and D'Asaro 1994). Existing knowledge in this geographic area is primarily based on strict applications of international mathematical developments, without any adjustment for the unique structure of the Mediterranean-type ecosystems and the implications of the local physicochemical and biological factors.

The goal of this work was to develop a consistent methodology for assessing nonpoint source pollution in the Mediterranean region. The effectiveness and the predictability of three models, the runoff curve number equation (CNE), the universal soil loss equation (USLE), and the mass response functions (MRF), were tested in a typical terrestrial ecosystem of the Mediterranean region. The study also provides the fundamental framework so that the requirements of the particular mathematical models are met, whereas conceptual modifications in the basic analysis of soil erosion and surface runoff are proposed with a view of improving the quantification of the nutrient outflows of the ecosystems. Finally, a critical discussion tends to emphasize the defects of these methods and the need for detailed sensitivity analysis and validation of these models under

various meteorological conditions, agricultural practices, and landscape characteristics of the Mediterranean area.

Methodology

The Study Area

This study was conducted within the gulf of Gera Basin, a 194-km^2 drainage area on the island of Lesvos (Figure 1). The flora on this island belongs to the *Oleo Ceratonion* zone. According to Thornthwaite's classification system, the local climate is of the type C_1dB_3' b_4', characterized by an annual rainfall between 600 and 800 mm; an annual evapotranspiration potential of 900 mm, and a high mean air temperature of 19°C (Arhonditsis and others 2000b). The area is considered as a typical terrestrial ecosystem of the Mediterranean region that is characterized mostly by shallow and infertile soils, steep slopes, water deficiency, and limited arable lands. The geological substrate consists mostly of metamorphic rocks (marbles, mica schists), igneous rocks (granites, basalts), and alluvial depositions. Most of the local rivers have a torrential regime that is considerably influenced by local precipitation characteristics and physiographic features of the area. Figure 2 illustrates the potential hydrographic characteristics of the watershed and shows that most of these flow paths
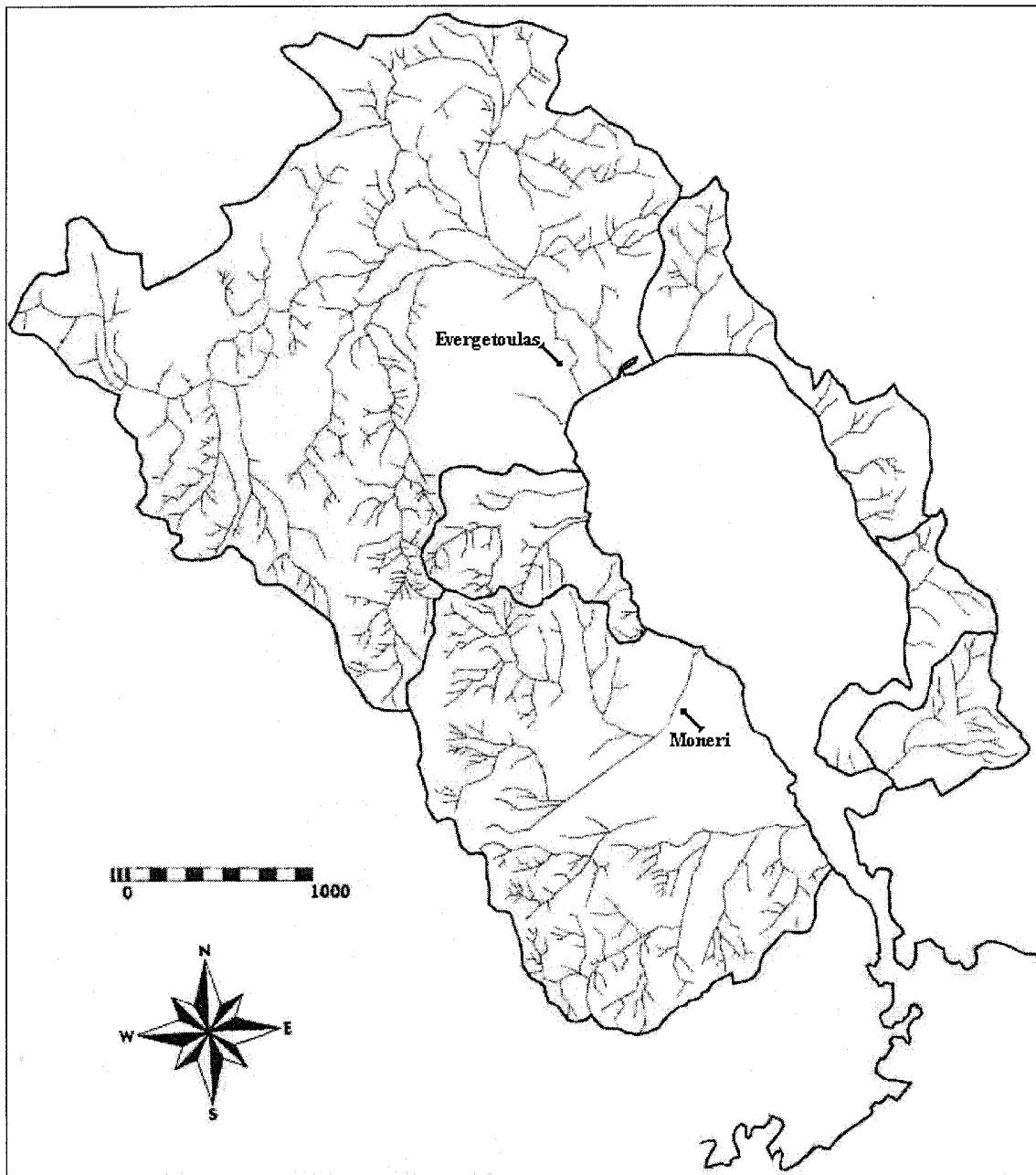
Figure 2. The hydrographic characteristics of Gulf of Gera's watershed.

usually remain inactivated but can occasionally contribute to the routing of the runoff volumes of storm events, especially during the years of high annual rainfall. Shortage of arable land in the watershed has been compensated by the construction of extensive systems of terraces that minimize soil erosion.

Table 1 lists the most abundant vegetation types of the area, as result of a landscape analysis based on the unsupervised and supervised classification of Landsat Thematic Mapper (TM) images (Hatzopoulos and others 1992). The landscape is characterized by a traditional monoculture of olive trees (*Olea europea*) occupying 60% of the total area of the watershed. Two types of olive plantations can be distinguished; cultivated and abandoned. Cultivated plantations are the olive groves in which cultivation takes place annually and wild woody plants are limited. Abandoned plantations are olive groves in

Table 1. Runoff curve numbers for hydrologic soil-cover complexes in catchment area of Gera (antecedent moisture condition II)

Land use or cover	Area (km²)	Treatment or practice	Hydrologic condition	Hydrologic soil group	Runoff curve number
Olive groves					
Cultivated	7.98	Terraced	Poor[a]	B	63
	23.59	—	Poor	B	65
	21.47	Terraced	Poor	C	72
	12.72	—	Poor	C	74
	9.95	Terraced	Poor	D	83
Abandoned	4.25	Terraced	Good[b]	B	52
	5.35	—	Good	B	54
	5.92	Terraced	Good	C	68
	13.55	Terraced	Fair[c]	C	71
	6.12	Terraced	Poor	C	75
	5.59	Terraced	Fair	D	77
Urban areas	8.37	—	—	C	88
Maquis	27.33	—	Poor	C	77
	37.09	—	Fair	C	74
Wetlands	6.73	—	Fair	D	79
Total	194.01				

[a]Poor hydrologic condition refers to areas that are heavily grazed or regularly cultivated so that litter, wild woody plants and brush are destroyed. The aboveground standing biomass of annual plants exceeds 50 g/m² dry wt (Arhonditsis and others 2000b).

[b]Good hydrologic condition refers to areas that are protected from grazing so that litter and shrubs cover the soil; whereas annual standing biomass is less than 20 g/m² dry wt.

[c]Fair hydrologic condition corresponds to the intermediate condition, i.e., areas that are not fully protected from grazing, and the annual standing biomass in the range of 20–50 g/m² dry wt.

which the canopy of the olive trees is limited, wild woody plants exist, and natural vegetation of olive trees has begun. The mountainous zones of the catchment (≈32%) are covered with evergreen sclerophyllous plant communities (maquis), phrygana in combination with coniferous trees (*Pinus brutia*), constituting the climax stage of natural ecosystems in the Mediterranean region. Furthermore, the landscape of the northwestern part of the watershed is characterized by the presence of wetlands (3.5%) used as pastures for sheep and goats year round. The structure and the dynamic behavior of these characteristic plant types of the Mediterranean region were studied by a dense sampling network (Figure 1), whereas the experimental procedure and further details about the results are reported elsewhere (Arhonditsis and others 2000b).

The subsequent seawater body, the gulf of Gera, is a semienclosed marine ecosystem with a mean depth of 10 m and a total volume of 9×10^8 m³. It is influenced by significant nutrient fluxes from agricultural runoff and soil erosion, especially during the winter period when the contribution is between 40% and 60% of the total nutrient flux (Arhonditsis and others 2000a). The chemical and biological information collected from eight sampling sites (Figure 1), revealed that the mean concentrations of nitrate,

phosphate, organic nitrogen, and chlorophyll are rather high, being 0.55, 0.19, 7.93 μg-at/liter and 0.98 μg/liter, respectively. These mean values are characteristic of a mesotrophic marine environment with eutrophic trends (Kitsiou and Karydis 1998). Thus, the potential threat for a further decline in the quality of the marine ecosystem indicates a need for the development of management schemes that control nonpoint pollution.

Application of Nonpoint Pollution Models

Inventory of source areas. Three nonpoint source pollution models were applied to the watershed to inventory its physicochemical and biological properties. This procedure was simplified considerably by the division of the heterogeneous and complex system into computational elements or grid cells. Cell size selection was investigated through sensitivity analysis of the models' input parameters (Vieux and Needham 1993), which indicated that in all cases the best fit with the experimental results was obtained using a grid of 0.25 × 0.25 km. The discrimination of the cell characteristics (i.e., soil type, land use, management or treatment practice, slope length, and distance from the nearest stream) was supported by the use of GIS (Hatzopoulos and others 1992). Nutrient variability, determined from the previous mentioned study, focused on the temporal patterns
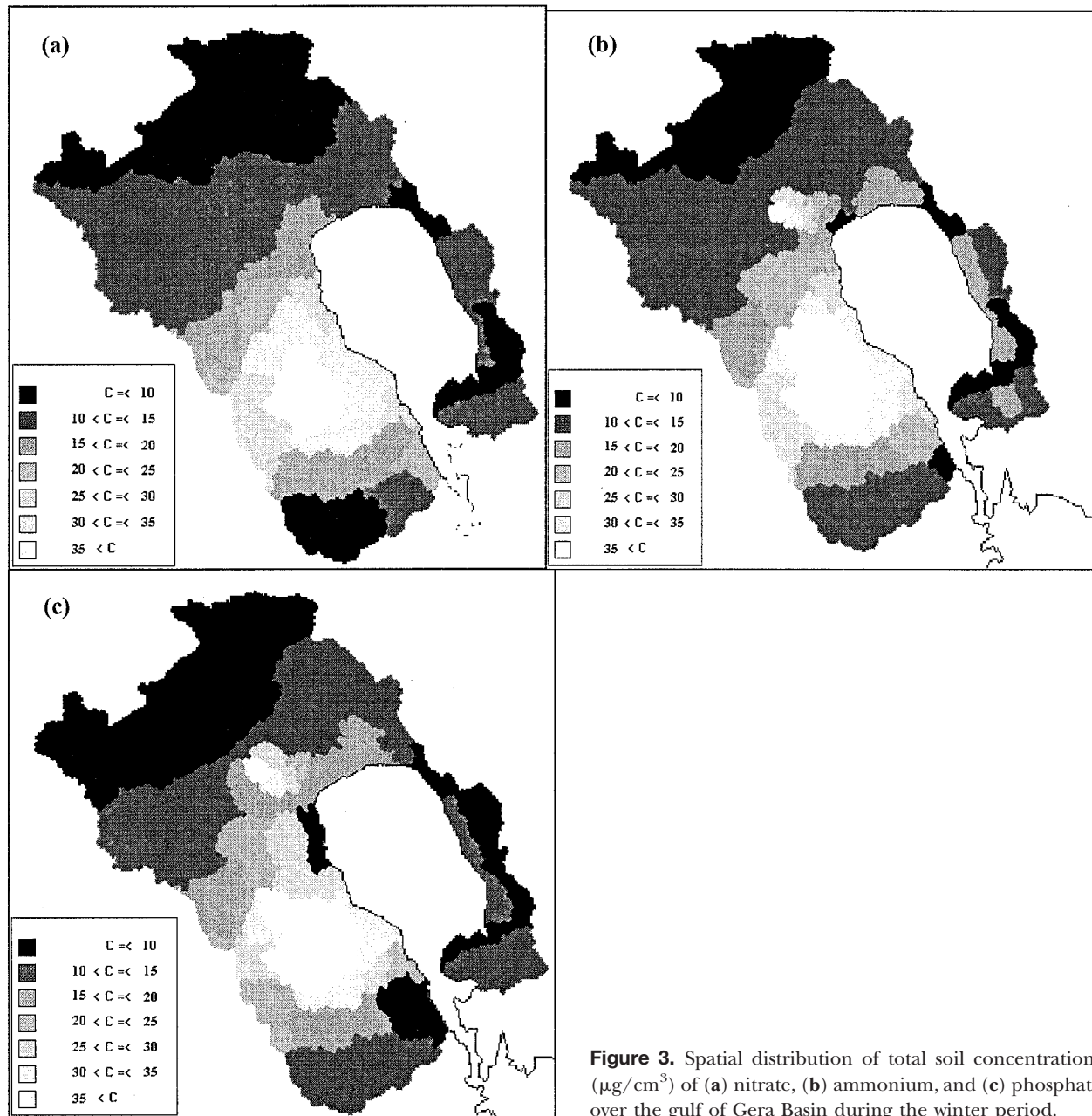
Figure 3. Spatial distribution of total soil concentrations ($\mu g/cm^3$) of (**a**) nitrate, (**b**) ammonium, and (**c**) phosphate over the gulf of Gera Basin during the winter period.

of inorganic nutrients and organic nitrogen over the most abundant vegetation types of the area (Arhonditsis and others 2000b). Figure 3 represents the spatial distribution of soil concentrations of nitrate, ammonium, and phosphate over the gulf of Gera basin during the winter period when the most significant rainfall events take place. The values of nutrients assigned to the intermediate cells that did not coincide with experimental sites (Figure 1), were obtained by interpolation using the inverse distance-weighting method (Watson and Philip 1985). The estimation of the solid and dissolved phase fraction was obtained through Langmuir (for phosphates) and Freundlich (for ammonium) isotherms, whereas the nitrate was assumed to be totally dissolved (Novotny and others 1978, Novotny and Chesters 1981). Daily and hourly precipitation records, used for the determination of the various model parameters, were available from a meteorological station located within the watershed.

Runoff curve number equation

Fundamental concepts. This method is a convenient means of estimating excess rain, and the general formulas describing the rainfall-runoff events are:

$$Q_{kt} = \frac{(R_{kt} - 0.2 \cdot S_{kt})^2}{2.54 \cdot (R_{kt} + 0.8 \cdot S_{kt})} \qquad (1)$$

$$CN_{kt} = \frac{1000}{10 + \dfrac{S_{kt}}{2.54}} \qquad (2)$$

in which R_{kt} is the rainfall (centimeters), on day t from source area k, S_{kt} is a detention parameter (centimeters), Q_{kt} is the runoff (centimeters), and CN_{kt} is an expression called "curve number," which is a tabulated function of soil hydrologic group, land cover, management, hydrologic condition, and antecedent soil moisture (Haith and Tubbs 1981). The term "soil hydrologic group" refers to the classification of the watershed soils into four hydrologic groups, according to their permeability and runoff potential (Chow and others 1988): group A contains soils with sands or gravel, exhibiting low surface runoff potential; groups B (moderately coarse texture) and C (moderately fine texture) present intermediate to slow rates of water transmission, respectively; and group D soils have high surface runoff potential, consisting chiefly of clay soils with a high swelling potential, soils with a permanently high water table, or shallow soils over nearly impervious material (Novotny and Chesters 1981).

The nutrient losses from a unit source area k, due to a runoff event on day t, are given by (Haith and Tubbs 1981):

$$LD = 10 \cdot Cd_{kt} \cdot Q_{kt} \cdot TD_k \qquad (3)$$

where LD_{kt} is the dissolved-phase fraction of nutrient loss in kilograms per square kilometer, Cd_{kt} is the nutrient concentration in dissolved phase measured in milligrams per liter TD_k is a transport factor indicating the fraction of dissolved-phase nutrient that moves from the edge of the source area to the watershed outlet, and Q_{kt} is the rainfall height in centimeters. The total dissolved nutrient export (LD) for a specific time period is calculated in equation 4, by multiplying the losses from each source by its respective area (A_k, in kilometer^2) and summing over all unit source areas and days in the time period:

$$LD = 10 \cdot \sum_t \sum_k Cd_{kt} \cdot Q_{kt} \cdot TD_k \cdot A_k \qquad (4)$$

Thus, the implementation of this method requires estimates of runoff, pollutant concentrations, and attenuation during the transport from each unit source area within the watershed.

Illustrative applications. One of the most important aspects of the model application was the determination of the runoff curve number values that correspond to the characteristic soil/cover complexes of the area (Hauser and Jones 1991). In the present work, the derived runoff curves were based on experimental results, extracted from the field plots of the sites in Figure 1. This network covered the entire extent of the watershed and took into consideration all the possible combinations of soil hydrologic groups, land uses or covers, and management and hydrologic conditions encountered in the study system. The size of the experimental plots was variable (10–26 m^2) and at least three repetitions per combination were used as a minimum standard of objectivity (Arhonditsis and others 2000b). Table 1 shows the results for the average soil moisture level of the area, the so-called antecedent moisture condition II (Novotny and Chesters 1981). Moreover, the effects of the antecedent soil moisture on the runoff curve values were obtained by the use of equation 5 (Hawkins 1978):

$$CN_2 = \frac{1200}{\dfrac{1200}{CN_1} + \dfrac{[ET - (R - Q)]}{2.54}} \qquad (5)$$

where CN_1 and CN_2 are the runoff curve values at times 1 and 2, respectively, R and Q are the interim rainfall inputs (centimeters) and runoff losses (centimeters), and ET is the sum of evapotranspiration and drainage losses (centimeters) during this time interval and were based on actual field measurements (Arhonditsis 1998). The minimal and maximal values of the runoff curves reflecting the lowest and the highest runoff potential of each unit source area, the so-called antecedent moisture conditions I and III, were based on the equations 6 and 7 (Chow and others 1988):

$$CN_I = \frac{CN_{II}}{2.334 - 0.01334 \cdot CN_{II}} \qquad (6)$$

$$CN_{III} = \frac{CN_{II}}{0.4036 - 0.0059 \cdot CN_{II}} \qquad (7)$$

where CN_I, CN_{II}, and CN_{III} are the runoff curve values of the three soil moisture classes.

The most fundamental factor affecting the concentrations of dissolved nutrients in runoff is the quantity of available nutrients in the soil. Although these nutrients may come from various sources, the total available nitrogen and phosphorus for a specific land cover is relatively constant and thus dissolved nutrient concen-

Table 2.   Dissolved ammonium, nitrate and phosphate,[a] concentrations in runoff from most abundant watershed land-cover categories of watershed

| | Concentrations (mg/liter) | | | | | |
| | Warm weather | | | Cold weather | | |
Land cover	Ammonium	Nitrate	Phosphate	Ammonium	Nitrate	Phosphate
Olive groves						
Cultivated	0.82 ± 0.15	1.21 ± 0.18	0.31 ± 0.08	0.61 ± 0.08	1.02 ± 0.12	0.22 ± 0.05
Abandoned	0.53 ± 0.09	0.72 ± 0.10	0.22 ± 0.07	0.30 ± 0.06	0.61 ± 0.05	0.20 ± 0.04
Urban areas	0.81 ± 0.18	0.81 ± 0.11	0.32 ± 0.10	0.81 ± 0.09	0.84 ± 0.08	0.34 ± 0.05
Maquis	0.21 ± 0.08	0.34 ± 0.08	0.12 ± 0.02	0.23 ± 0.03	0.19 ± 0.04	0.15 ± 0.02
Wetlands	0.62 ± 0.17	0.72 ± 0.12	0.29 ± 0.05	0.50 ± 0.04	0.58 ± 0.10	0.20 ± 0.03

[a]Refers to all the filterable molybdate-reactive P.

trations in runoff are primarily functions of the vegetation types in the source areas (Scholefield and Stone 1995, Summers and others 1999). Table 2 shows flow-weighted average dissolved ammonium, nitrate, and phosphate concentrations in runoff from the most abundant plant types of the watershed, measured on the field plots over three years of natural precipitation. Since average nutrient concentrations often differ significantly over the year, the concentrations were separated into cold- and warm-weather categories in order to increase model accuracy. Given the climatic conditions of the Mediterranean region, cold-weather conditions were assumed to last from the first day in which the 30-day running average temperature fell below 10°C (early December) until the first day in which the 30-day average exceeded 10°C (the end of February or early March). The warm-weather concentrations are higher as a result of fertilizer applications and microbial activity, accelerated by the favorable abiotic factors (temperature, solar radiation, moisture) that prevail during this time period (Moreno and Oechel 1995).

Numerous applications of the CNE are based on the assumption that both runoff and dissolved pollutants are conserved during their movement from the farmer's fields to the watershed outlet. This perception is valid for dissolved substances (i.e., nitrates) that are attenuated primarily by biological phenomena and thus are not likely to be significantly reduced (Haith and Tubbs 1981). Consequently, a transport factor equal to 1 was considered for dissolved losses of nitrate for all the unit source areas of the watershed. On the other hand, there may be opportunities for dissolved chemicals such as phosphate and ammonium to be removed from the runoff solution by adsorption or by chemical reactions with the topsoil. In these cases, the assumption that $TD_k = 1$ would be invalid, especially for single isolated events, leading to overestimation of the export of dissolved pollutants from watersheds. Thus, a new transport factor for phosphate and ammonium was applied, given by equation 8:

$$TD_k = e^{-\alpha \cdot d_k} \tag{8}$$

where d_k is the downslope distance (meters) from the center of source area k to the nearest identifiable drainage channel, and α is a coefficient, which was found, after model calibration, to be 0.001 for ammonium and 0.002 for phosphate.

Mass response functions

Fundamental concepts. The mass response functions are defined as probability–density functions associated with the random holding time of the water particles within the basin and conditional on the time of occurrence of the storm event. The particle-holding times are assumed to drive mass transfer through contact between phases and control the chemical process of sorption phenomena (Rinaldo and Marani 1987). The fundamental model structure may be described as the combination of a water quality component, based on a simple mass balance, with the Nash conceptual hydrologic model of rainfall–runoff transformations (Bendoricchio and Rinaldo 1986). The latter component models the watershed as a cascade of continuously stirred tank reactors. According to this concept, the transfer function of a hydrologically active unit area to rainfall events distributed in time according to $i(\tau)$ is built by convolution as:

$$Q(t;n;k) = \int_0^t h(t-\tau;n;k) \cdot i(\tau)\,d\tau \tag{9}$$

where

$$h(t;n;k) = \frac{1}{k \cdot \Gamma(n)} \cdot (t/k)^{n-1} \cdot e^{-t/k} \tag{10}$$

where $Q(t;n;k)$ is the flow output (cubic meters per hour) per unit source area (square meters), $h(t;n;k)$ is the ordinate of the instantaneous unit hydrograph (hours^{-1}), τ is the lag time that corresponds to the time interval between maximum rain excess and the peak of the runoff (hours), $i(\tau)$ is the impulse hyetograph (meters per hour), n is a dimensionless watershed characteristic representing approximately the number of reservoirs, (n) is the gamma function of n, and k is a storage constant (hours^{-1}) related to the time of travel of rainwater from the most remote point on the watershed to the watershed outlet t_e (time of equilibrium or time of concentration) by the expression $k = t_e/n$.

Furthermore, the conceptual scheme for the chemical mass transfer, in a continuously stirred tank reactor, is given by:

$$\frac{\partial c}{\partial t} = h(c_e - c) \qquad (11)$$

where c is the current nutrient concentration (miligrams per liter) in the runoff volume (mobile phase), c_e is the equilibrium concentrations (miligrams per liter) in the dissolved-phase (an interphase where solid or fixed and mobile phases are in equilibrium), and h is a mass transfer coefficient (hours^{-1}) that measures the actual speed of chemical transfer from the interphase to the bulk of the runoff (Zingales and others 1984). In the case that c_e is a time-independent variable and h is a spatial and temporal constant, the flow rate q of a nutrient and the total quantity Z in the watershed outlet, are given by the following unit-mass response functions:

$$q(t;\ n;\ k;\ h;\ c_e') = c_e' \cdot \left\{ Q(t;\ n;\ k) \right.$$
$$\left. - \left(\frac{k}{k+h}\right)^n \cdot Q(t;\ n;\ k\ +\ h) \right\} \quad (12)$$

$$Z(t;\ n;\ k;\ h;\ c_e') = \int_0^t q(t;\ n;\ k;\ h;\ c_e')\,dt = c_e' t \cdot \left\{ V(t;\ n;\ k) \right.$$
$$\left. - \left(\frac{k}{k+h}\right)^n \cdot V(t;\ n;\ k+h) \right\} \quad (13)$$

$$c_e' = \int_{y_1}^{y_2} \int_{x_1}^{x_2} c_e'(x,\ y)\,dx dy \qquad (14)$$

where $q(t;n;k;h;c_e')$ is the nutrient flow rate (miligrams per hour), $Z(t,n,k,h,c_e')$ is the total nutrient load (miligrams) at time t, $Q(t;n;k)$ is the flow output (m^3 per hour) and $V(t;n;k)$ is the runoff volume discharge (cubic meters) at time t per unit area (square meters).

Finally, the term c_e' constitutes an innovation of the present study, referring to the spatial variability of c_e' over the basin. It is computed by integrating the distribution function $c_e(x,y)$ of the dissolved-phase concentrations over the catchment area, where x_1, x_2, y_1, and y_2 correspond to the coordinates of the watershed boundaries.

Illustrative applications. One principal question of the model application is how many linear pools are needed for the simulation of solute transport in the hydrologic response (Bendoricchio and Rinaldo 1986). In the present work, the optimum fitting between computed runoff and measured hydrographs was produced by applying $n = 2$. Furthermore, the estimation of the scale parameter k was sought from two alternative methods in the literature; the parameterization of the instantaneous unit hydrograph in terms of Horton order ratios or the application of Manning's surface roughness factor-based equations to compute the time of equilibrium (Novotny and Chesters 1981, Rosso 1984, Chow and others 1988). Given the ambiguous hydrographic status of the study watershed and the torrential regime of the local rivers, the determination of some essential input requirements of the former approach, such as the geomorphologic characteristics of the basin (i.e., the Horton's numbers R_A, R_B, and R_L or the mean length of ith order stream), is rather complicated and inaccurate. Thus, the latter method is deemed more appropriate and reliable for areas characterized by the geomorphoclimatic conditions of the Mediterranean region. The estimation of the time of equilibrium t_e for each source area was computed by the following formulas:

$$t_e = t_{e1} + t_{e2} \qquad (15)$$

$$t_{e1} = 6.9 \cdot \frac{L_1^{0.6} \cdot n_{M1}^{0.6}}{i^{0.4} \cdot S_1^{0.3}} \qquad (16)$$

$$t_{e2} = 0.017 \cdot \frac{L_2 \cdot n_{M2}}{R^{2/3} \cdot S_2^{0.5}} \qquad (17)$$

where t_{e1} and t_{e2} are the time lengths (minutes) of the overland and channel flow, respectively, i the rain intensity (millimeters per hour), R is the hydraulic radius (meters) of the channel defined as cross-sectional area divided by the wetted perimeter, S_1 and S_2 are the mean slopes (meters per meter) of the overland and channel flow, L_1 and L_2 are the lengths (meters) of the overland and channel flow, n_{M1} and n_{M2} are the Mannings surface roughness factors, which vary with the ground cover. Table 3 presents literature-based values of the Manning factors (Chow and others 1988), adjusted during the calibration process in order to obtain better

Table 3. Mean values of the Manning's roughness factor, n_M, for overland and channel flow over study watershed[a]

	Manning's roughness factor (n_M)
a) Overland flow	
Olive groves	
Cultivated, ground cover	
> 60%	0.28
30–60%	0.22
< 30%	0.16
Abandoned, ground cover	
>50%	0.38
<50%	0.32
Maquis, ground cover	
>70%	0.18
35–70%	0.12
<35%	0.08
Channel flow	
Earth, straight and uniform	0.028
Earth and winding	0.042
Few trees, stones, or brush	0.063
Weeds and stones	0.055

[a]Literature-based values of Manning factors (Chow and others 1988), adjusted during the calibration process.

fit between simulated and experimental data. These values can also be extrapolated and tested in other catchments of the Mediterranean region characterized by the same land uses or ground covers with similar qualitative characteristics and species composition. The first equation of the overland flow was developed for a two-plane V-shaped watershed using the kinematic wave approximation, but can account for wider and more complex representations after the division of the watershed into homogeneous computational elements (Chow and others 1988). On the other hand, the second equation presumes a uniform flow of runoff in the open channels, a prerequisite that seems to be valid, since the depth of flow in the local torrents and rills is approximately constant in the direction of flow (Albertson and Simons 1964).

Another critical point of the model development was the incorporation of the term c'_e that describes the spatial variability of the dissolved-phase concentrations of nitrate, ammonium, and phosphate over the basin. This addition amplifies the role of the features of the study system in the modeling procedure, resulting in more realistic results (Bendoricchio and Rinaldo 1986, Rinaldo and Marani 1987). The description of the equilibrium concentrations c'_e as a function of space was obtained in two ways: (1) the interpolation method, computing the spatial heterogeneity of dissolved-phase

nutrients, similar to the method already used for the total soil concentrations, and (2) multiple regression analysis (Draper and Smith 1981). In this particular case, a preliminary test (not reported in this paper) showed that the later approach produced a better fit between observed and computed values, and it was therefore considered more suitable for the explicit expression of the mass response functions. The watershed was divided into six subcatchments (outlined in Figure 2), where separate sets of equations were formed in order to increase accuracy of the method (Arhonditsis 1998). Seasonality effects (i.e., variations of c_e at time scales larger than that of the hydrologic response) were also taken into account by defining three (four seasons minus one) dummy variables (Golfinopoulos and others 1998). The seasons with the dummy variables were winter (win), spring (spr) and autumn (aut). As an example, the values of the variable (win) were determined by the expression:

$$\text{win} = \begin{cases} 1 & \text{if the simulated runoff event takes place in the winter period} \\ 0 & \text{otherwise} \end{cases}$$

Preliminary data analysis involved the testing of normality using the Kolmogorov-Smirnov test and data transformations in the cases of a poor fitting to the normal distribution. The data were also tested for homoscedasticity using the Durbin-Watson test, whereas the relationships between the variables were examined by simple correlation (Vounatsou and Karydis 1991). The equations describing the spatial distribution of the dissolved-phase concentrations of nitrate, ammonium, and phosphate over the western part of the basin (similar equations were developed for the rest parts of the watershed), are the following:

$$NO_{3(e)} = 44.3868 \cdot x + 32.0318 \cdot y$$
$$+ 6.3751 \cdot win \cdot y + 14.9041 \cdot spr$$
$$- 11.1821 \cdot x \cdot y - 5.4032 \cdot x^2 \quad (18)$$

$$NH_{4(e)} = 0.3551 \cdot x + 0.7564 \cdot y^2 + 0.3790 \cdot win \cdot y$$
$$+ 0.3113 \cdot spr - 0.3066 \cdot x \cdot y \quad (19)$$

$$\log PO_{4(e)} = 0.2272 \cdot x + 0.1492 \cdot y$$
$$+ 0.0344 \cdot win \cdot \sqrt{y} + 0.0209 \cdot spr$$
$$- 0.3555 \cdot x \cdot y \quad (20)$$

$$0.15 \leq x \leq 5.6 \text{ km} \text{ and } 0.01 \leq y \leq 1.5 \text{ km}$$

where the ranges of the variables x and y are defined by the coordinates of the remotest experimental sites along the two dimensions of the basin. Generally, the method has resulted in statistically significant regres-

sion models at the 5% level, with satisfactory multiple determination coefficients ($R^2 \geq 0.75$) for all subcatchments of the watershed (Arhonditsis 1998).

The calibration of the model was obtained by systematic sampling and flow measurements on an hourly basis during the occurrence of several rainfall–runoff events. The samples were taken from the outlets of the two basic torrents of the area, located on the northern and western part of the watershed. Analytical work was focused on the determination of nitrate, ammonium, and phosphate concentrations in the bulks of runoff (Arhonditsis 1998). Finally, the lack of experimental measurements of the base flow for some rainfall events was overcome by the hydrograph separation technique, based on drawing a straight line from the point of rise to a point on the lower portion of the recession segment of the hydrograph (Chow 1964).

Universal Soil Loss Equation

Fundamental concepts. The universal soil loss equation (USLE) is the most common estimator of soil loss caused by upland erosion and when applied to individual rainstorms it is formulated as:

$$X_{kt} = R_t \cdot C_k \cdot K_k \cdot L_k \cdot S_k \cdot P_k \qquad (21)$$

where X_{kt} is soil erosion (tons per hectare) on day t from source area k, C_k is the crop management factor (unitless), which reflects the effects of cropping and management practices on erosion rates, K_k is the soil erodibility factor, (tons $\cdot$ hectare $\cdot$ hours)/(hectare $\cdot$ megajoules $\cdot$ centimeters), which is an estimate of the potential erodibility of the soil, P_k is the erosion control practice factor (unitless), which accounts for the erosion control effectiveness of various land treatments or control structures, L_k is the slope length factor (unitless), and S_k is the steepness factor (unitless), which represents the effects of overland runoff length and slope steepness on erosion (Yoder and Lown 1995). The remaining term R_t is the rainfall energy intensity factor (megajoules $\cdot$ centimeters per hectares $\cdot$ hours) for the rainstorm on day t, based on the following formulas (Bagarello and D'Asaro 1994):

$$R_t = 0.013 \cdot E_t \cdot I_t^{30} \qquad (22)$$

$$E_t = \sum_{i=1}^{n} E_i = 10 \cdot \sum_{i=1}^{n} [206 + 87 \cdot \log_{10}(I_i)] \cdot r_i$$

$$(23)$$

in which I_t^{30} is the maximum 30-min storm intensity (centimeters per hour), E_t is the storm kinetic energy (megajoules per hectare) computed by dividing the rainfall into n intervals of constant intensity, and E_i, I_i,

r_i are the kinetic energy. (megajoules per hectare), the intensity (centimeters per hour), the total rain (centimeters) of the ith interval, respectively. In the present work, given the precipitation characteristics of the Mediterranean region (relatively small duration, rapid changes in the intensity), the rainfall events were divided into 15-min intervals.

The nutrient losses from unit source area k, due to soil erosion on day t, are given by (Haith and Tubbs 1981):

$$LS_{kt} = 0.1 \cdot Cs_{kt} \cdot X_{kt} \cdot TS_k \qquad (24)$$

where LS_{kt} is the solid-phase fraction of nutrient loss in kilograms per kilometer^2, Cs_{kt} is the nutrient concentration in solid-phase form measured in milligrams per kilogram, TS_k is a transport factor indicating the fraction of solid-phase nutrient that moves from the edge of the source area to the watershed outlet, and X_{kt} is the soil loss (tons per hectare). The total solid nutrient export (LS) for a specific time period is calculated by multiplying the losses from each source unit area by its respective area A_k (in kilometers^2) and summing over all unit source areas and days in the time period:

$$LS = 0.1 \cdot \sum_t \sum_k Cs_{kt} \cdot X_{kt} \cdot TS_k \cdot A_k \qquad (25)$$

This method requires estimates of erosion, pollutant concentrations, and attenuation during the transport from each unit source area to the watershed outlet.

Illustrative applications. The estimation of the crop management (C), soil erodibility (K), and erosion control practice (P) factors, was based on three years of experimental field results from the sites in Figure 1. Arhonditsis and others (2000b) evaluated all possible combinations of soil texture, organic matter content, land cover, topographic features, and management practices encountered in the study watershed. Table 4 shows the experimental mean values and the respective standard deviations of these factors for various subclasses, discriminated in terms of the percentage tree canopy, ground cover, organic matter content, and slope. These subclasses were statistically significant groups with regard to the factor values, defined (i.e., ranges, upper and lower limits) by forming different combinations of groups with varying sizes and limits and testing their significance with parametric or nonparametric analysis of variance (Zar 1984). Additionally, mathematical expressions and parameters describing the slope-length and the slope-steepness factors are presented in Table 5 (Moore and Wilson 1992, Renard and others 1994).

Concentrations of solid-phase nutrients in eroded soil (sediment) usually exceed these of in situ soil, since

Table 4.   Mean values of crop management, soil erodibility, and erosion control practice factors of universal soil loss equation[a]

Land cover	Crop management factor (C)	Soil erodibility factor (K)		Erosion control practice factor (P)	
		Western part of the watershed (mean soil texture; sandy loam)			
Olive groves				*Terracing*	
Cultivated, tree canopy		OM ≤ 1.0	0.28 ± 0.02		
>60%	0.008 ± 0.002	1.0 < OM ≤ 2.0	0.25 ± 0.02	S ≤ 5.0	0.20 ± 0.01
30–60%	0.012 ± 0.003	2.0 < OM ≤ 3.0	0.22 ± 0.02	5.0 < S ≤ 10.0	0.25 ± 0.02
<30%	0.020 ± 0.004	3.0 < OM ≤ 4.0	0.20 ± 0.02	10.0 < S ≤ 15.0	0.30 ± 0.02
		Northern part of the watershed (mean soil texture: silty loam)		15.0 < S ≤ 20.0	0.35 ± 0.01
				20.0 < S ≤ 25.0	0.45 ± 0.01
Abandoned, ground cover		OM ≤ 1.0	0.47 ± 0.04	25.0 < S ≤ 30.0	0.55 ± 0.03
>50%	0.005 ± 0.002	1.0 < OM ≤ 2.0	0.43 ± 0.03	30.0 < S ≤ 35.0	0.70 ± 0.02
<50%	0.010 ± 0.002	2.0 < OM ≤ 3.0	0.38 ± 0.02	35.0 < S	1.00 ± 0.02
		3.0 < OM ≤ 4.0	0.34 ± 0.03		
		Eastern part of the watershed (mean soil texture: sandy clay)		*No erosion control practices*	
Maquis, ground cover		OM ≤ 1.0	0.15 ± 0.01	Factor P = 1.00	
70%	0.211 ± 0.021	1.0 < OM ≤ 2.0	0.14 ± 0.03		
35–70%	0.308 ± 0.022	2.0 < OM ≤ 3.0	0.13 ± 0.02		
<35%	0.501 ± 0.025	3.0 < OM ≤ 4.0	0.12 ± 0.01		

[a]OM represents the organic matter Content (%) of the soils.

[b]S represents the slope (%).

Table 5.   Mathematical expressions and parameters describing slope–length and slope–steepness factors of the universal soil loss equation (Moore and Wilson 1992, Renard and others 1994)

Equations	Parameters
$L_k = [\lambda_k/22.13]^{m_k}$	L, Slope–length factor λ_k, the horizontal slope length (m) parameter of a source area k, extracted from contour maps m_k, an exponent related to the ratio of rill erosion (caused by flow) to interrill erosion (principally caused by raindrop impact) S, slope-steepness factor
$S_k = \begin{cases} 3.0\sin\theta_k^{0.8} + 0.56 & slope_k < 4.5\% \\ 10.8\sin\theta_k + 0.03 & 4.5 \le slope_k < 9\% \\ 16.8\sin\theta_k - 0.5 & slope_k \ge 9\% \end{cases}$ $\theta_k = \arctan slope_k(\%)/100$	

erosion and sediment transport processes selectively favor the small organic matter and clay particles that contain much of the soil's nutrients (Renard and Ferreira 1993). Thus, in situ soil nutrient concentrations are multiplied by an enrichment ratio to estimate concentrations in the sediment. Enrichment ratio studies have been reviewed by several investigators, but the only conclusions that can be drawn are that enrichment ratios for N and P typically vary from 1 to 4 (Culley and Bolten 1983, Dorioz and others 1989, Alexander and others 2000). In the present work, the experimental procedure revealed that the concentrations of ammonium and phosphate in sediment were approximately twice the concentrations of the in situ soil (Arhonditsis) (and others 2000b), which is also the most frequent value reported in the literature (Smith and Patrick 1991, Sheridan and others 1999).

Solid-phase nutrients move with sediments, and therefore transport factors for sediment losses or sediment delivery ratios can be used directly. The present study has
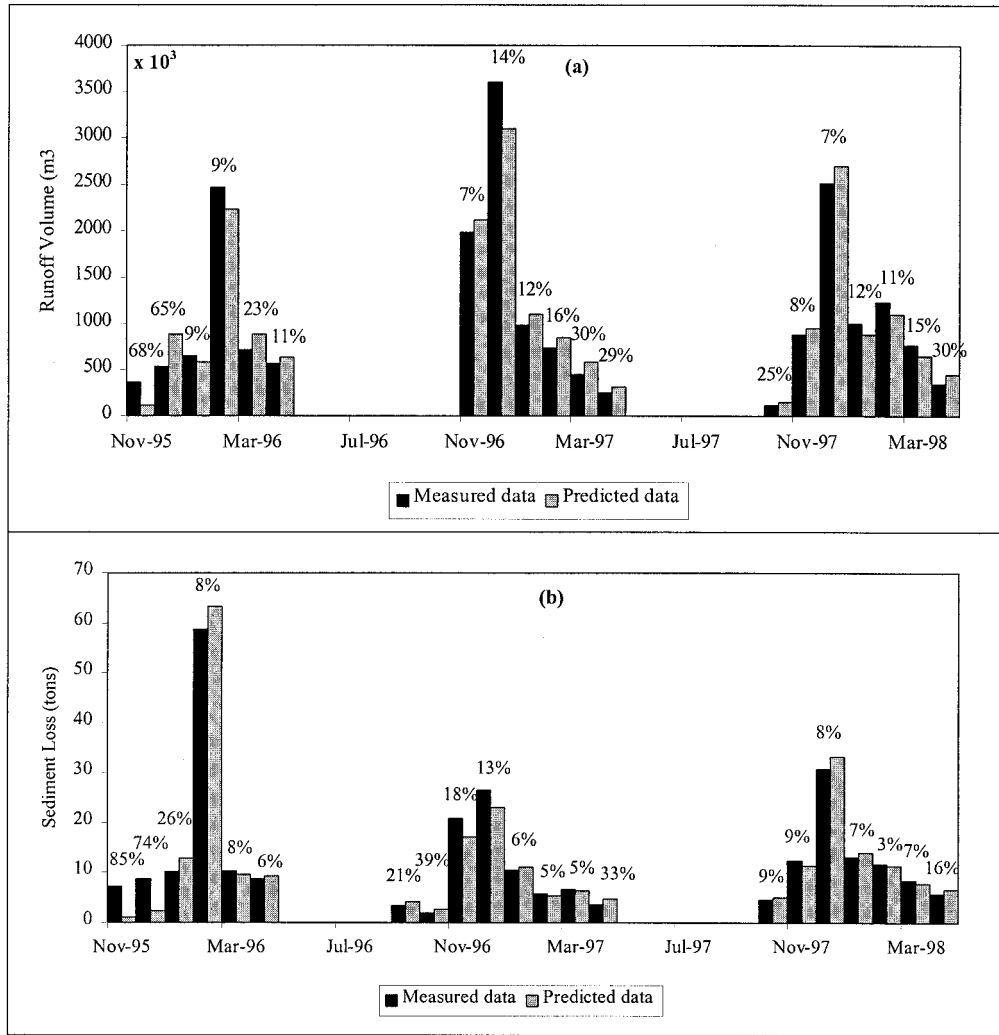
Figure 4. Measured versus predicted cumulative monthly (**a**) runoff volumes and (**b**) sediment losses from Gera's watershed. The simulated data are based on the use of the Runoff Curve Number Equation and the Universal Soil Loss Equation, respectively. The experimental data result from extrapolation of field measurements on unit plots (Arhonditsis and others 2000b). As a deviation measure between experimental and simulated data was used, the absolute percent error (APE = 100 × Π observed value − simulated value Π/observed value).

selected a delivery ratio sensitive to the location of source areas with respect to streams; a feature that permits the identification of fields with the greatest sediment delivery ratios and enables the evaluation of control techniques and management structures on specific places of the watershed (Novotny and Chesters 1981):

$$TS_k = d_k^{-0.34} \qquad (26)$$

where TS_k is the sediment delivery ratio for field or unit source area k, and d_k is the downslope distance (meters) from the center of source area k to the nearest identifiable drainage channel. The exponent value −0.34 was

a result of the calibration of the model, giving the best fit with experimental data.

Results and Discussion

Runoff Curve Number Equation

Simulated and observed monthly runoff from Gera's watershed during the period of the experiment is shown in Figure 4a. Direct runoff was computed as the total streamflow volume for an event minus the respective baseflow, which in turn was identified using the previously described hydrograph separation technique.

It can be seen that the absolute percent error (APE) was less than 30% for the entire simulation period aside from November and December of 1995, which were the only exceptional cases. In general, most of the runoff discharges occurred from November to April, and December seems to be the wettest month of year with a cumulative runoff volume that reaches or sometimes exceeds 3 million cubic meters. On the other hand, rainfall–runoff events during the summer period are rare, and the watershed soils are dry, characterized by a moisture content that can occasionally approach the wilting point. Such an extreme and prolonged period of drought occurred from the summer until the late autumn of 1995, resulting in soil moisture levels below the presumed lowest limit of moisture class I. In this period, the assignment of runoff curve values to the soils was inaccurate, leading to major discrepancies between simulated and experimental data after the occurrence of the first runoff events in November (68%) and December (65%) of 1995. The results improved significantly in January of 1996 (9%), when soil moisture and general hydrological activity of the watershed ranged within the limits and model assumptions.

Similar inferences could be extracted from dissolved-phase nitrate, ammonium, and phosphate, since predicted exports from the study watershed are proportional to runoff. Figure 5 shows that the model closely reproduces the annual trends of dissolved-phase nutrient losses. Nonpoint nutrient loading was significant during the winter period, whereas the summer losses into the subsequent seawater body were negligible. The maximum monthly values were observed in February 1996, when a number of storm events resulted in extreme losses of 9.6, 4.5, and 3.3 tons of nitrate, ammonium, and phosphate, respectively. Moreover, the highest nutrient concentrations in the runoff volumes were noted during February and March, mainly due to contemporary application of fertilizers to the olive groves.
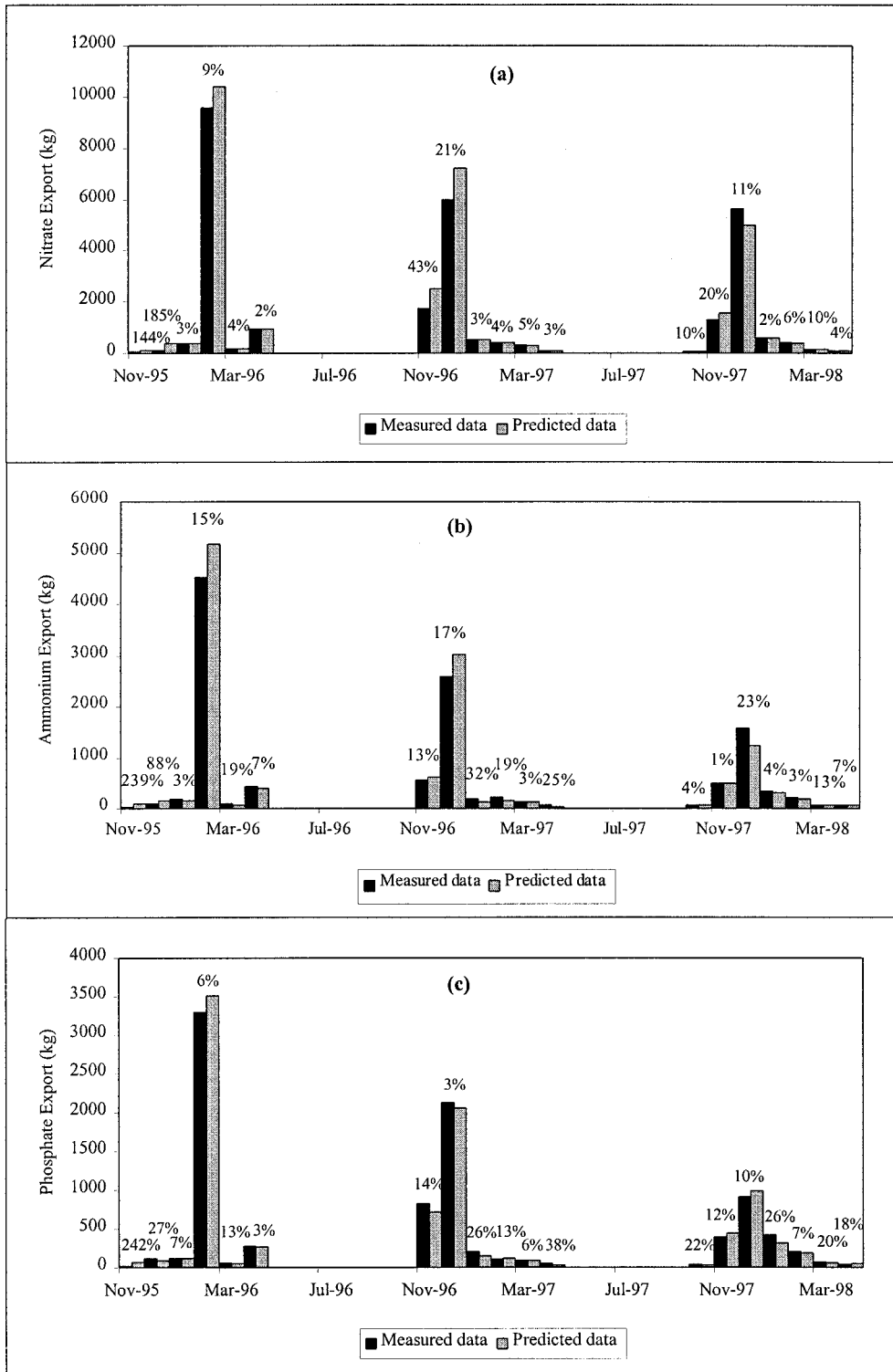
It seems the runoff curve number equation accurately simulates rainfall–runoff processes and should be considered an effective method for predicting dissolved-phase nutrient fluxes over the study watershed. The estimated curve numbers (Table 1) and the nutrient concentrations in the runoff (Table 2) can be proposed as reference values for similar works in basins characterized by land uses, management practices, and hydrologic conditions of the Mediterranean region. Moreover, the new formula for the transport factor accurately reproduces the transport of dissolved ammonium and phosphorus within the watershed. However, the nonuniform distribution of rainfall over the annual cycle and the extended dry periods that frequently characterize the Mediterranean climate lead to extreme conditions that cannot be described adequately by this method. The runoff curve number technique was not generated to account for moisture levels lower than those of the dry soils of the so-called antecedent moisture condition I (Chow and others 1988). This shortcoming could be overcome by redefining the lowest limits of the runoff curve numbers for the specific combinations of soil hydrologic groups, land covers, management, and hydrologic conditions. Such an adjustment requires experimental data similar to those obtained during November and December of 1995, but also a broader framework and testing of the results in additional locations of the Mediterranean area. Finally, the runoff processes due to snowmelt were not considered, since the occurrence of such events is rare and insignificant in the islands of the Aegean Sea.

Mass Response Functions

The application of this mathematical model, based on conditional probabilistic schemes, was intended to diminish the study time-scale of event-based responses to instantaneous intertidal values, in order to effectively integrate terrestrial loading with contemporary retention time in the recipient gulf. Such a time scale is deemed necessary during periods when the hydrodynamic regime favors the rapid export of excessive nutrient loads into the open sea and the seawater is renewed in time spans of less than ten days (Arhonditsis and others 2000a). Figure 6 illustrates experimental and simulated flow rates of nitrate, ammonium, and phosphate at the outlet of the Evergetoulas River over a number of extreme rainfall events that took place from 25 November to 3 December 1996. The presentation of this particular case was due to its unique and extreme character, since such a sequence of storm events resulting in a total runoff discharge of 1.5×10^6 m^3, occurs once or twice a decade. It can be seen that the model accurately predicted the flow rates of dissolved-phase nutrients. Minor discrepancies were observed after the fifth day when a heavy and protracted storm had led to tenfold (phosphate) and 40-fold (nitrate) increases of the nonpoint fluxes. Similar inferences could be extracted from the rest of the simulated rainfall–runoff events, where their milder characteristics (intensity, time duration) resulted in a better agreement with the experimental measurements.

The quantitative assessment of the goodness-of-fit between experimental and simulated flow rates of dissolved-phase nitrate, ammonium, and phosphate for 12 storm events was performed by the two-sided Kolmogorov-Smirnov test (Table 6). This statistical analysis checks the maximum difference between simulated and observed distributions to determine if it exceeds a

Figure 5. Measured versus predicted cumulative monthly exports of dissolved-phase (**a**) nitrate, (**b**) ammonium, and (**c**) phosphate from Gera's watershed. The simulated data are based on the use of the Runoff Curve Number Equation. The experimental data result from extrapolation of field measurements on unit plots (Arhonditsis and others 2000b). As a deviation measure between experimental and simulated data was used the absolute percent error (APE = 100 × Π observed value − simulated value Π/observed value).

critical value. Its nonparametric character has a much higher power than normal statistical techniques (i.e., t test, regression analysis) for analyses of data sets involving small sample sizes and skewed distributions, i.e., the monitored storm load data sets (Hartigan and others 1983). Based on a 0.05 probability cutoff for the 95% confidence interval, the statistics in Table 6 indicate that the simulated nutrient loads do not vary significantly from those monitored in the watershed. It can also be observed that this model accounts for a wide range of rainfall–runoff events, including surface nutrient wash-off loads from a few kilograms up to 2000 kg or more. However, the simulation of two rainfall events that took place in December 1995, after the dry autumn of 1995, was unsuccessful and resulted in significant deviations from the observed data (results not presented in this paper). These inaccuracies were attributed mostly to erroneous estimations of the net rainfall over time, since the leaching in such an extreme level of aridity seems to be more complex and unpredictable than in the usual situations (Bai and others 1996).

Finally, the mass transfer coefficient h had a critical role for the simulation process, varying from event to event (0.03–0.26 hours^{-1}) and thus modifying the shape, timing, and ordinates of the pollutants' runoff impulse. The physical interpretation of this coefficient includes the contributions of several microscopic mechanisms, depending on (1) the physics of the transport phenomena involved, (2) the geometry of the microscopic contact, and (3) the chemical components involved; moreover, the present work has revealed a potential relation between its values and the ambient temperature (Rinaldo and Marani 1987, Arhonditsis 1998). These inferences constitute an aim of on-going research to develop mathematical expressions that link the factor h with physicochemical parameters and clarify the transfer processes from the interphase (where fixed and mobile phase are in equilibrium) to the runoff bulks.

Universal Soil Loss Equation

Predictions of monthly sediment losses and the respective APEs over the testing period are illustrated in Figure 4b. The model closely reproduces the monthly sediment loss and demonstrates that significant quantities of soil are lost in the winter period (50–80 tons), whereas in the summertime the losses were negligible.

The model accurately predicted the occurrence of two large sediment-yielding months—February 1996 (58 tons) and December 1997 (31 tons). Time lags between erosion and sediment delivery, reflecting the deposition and resuspension components of the sediment transport process, were minor due to the steepness of the study watershed. As a consequence of this feature, the accuracy of event-based simulations of soil erosion has increased, and this would enable the development of integrated modeling approaches that focus on the downstream conditions that link terrestrial and aquatic processes. (The perspectives for event-based simulations are discussed in the Summary and Conclusions section below).

The USLE has also presented inaccurate predictions under extreme conditions of dryness, underestimating soil erosion during November–December 1995. Initially the APE for these months was 137% and 122%, respectively (not included in Figure 4b). By contrast with the previous models, the specific procedure has the capability to surpass this problem by changing the value of the exponent m (initially $m = 0.60$) of the slope length factor L. As was shown in Table 5, this exponent is a tabulated function of the percent slope and the rill (caused by flow) to interrill (principally caused by raindrop impact) ratio of the source areas. In general, the watershed is characterized by consolidated soils with little to moderate cover associated with an intermediate rill–interrill ratio. However, these conditions change drastically during the period of aridity when the annual plants, effective in preserving soil cohesiveness, could not be sustained by the low moisture content (Crubb and Hopkins 1986). Consequently, the unconsolidated character of the soils led to a high ratio of rill to interrill erosion, increasing the values of the exponent m (a value of $m = 0.72$ gave the best results), which in turn relatively improved the simulations of the watershed's behavior during the first rainstorms after the dry period. (The APE for November and December of 1995 decreased to levels of 85% and 74%, respectively).

The model also accurately described the temporal variations of solid-phase ammonium and phosphate exports from the study watershed (Figure 7). Moreover, in terms of coastal management and soil and water conservation, the model was effective in simulating nutrient losses from the various ecosystems of this Mediterranean area. It was predicted that nutrient fluxes via

Figure 6. Flow rates of nitrate, ammonium, and phosphate for a sequence of rainfall events that took place from 25 November to 3 December 1996: experimental and simulated data, based on the use of the Mass Response Functions, at the outlet of the most important torrent of Gera's watershed.
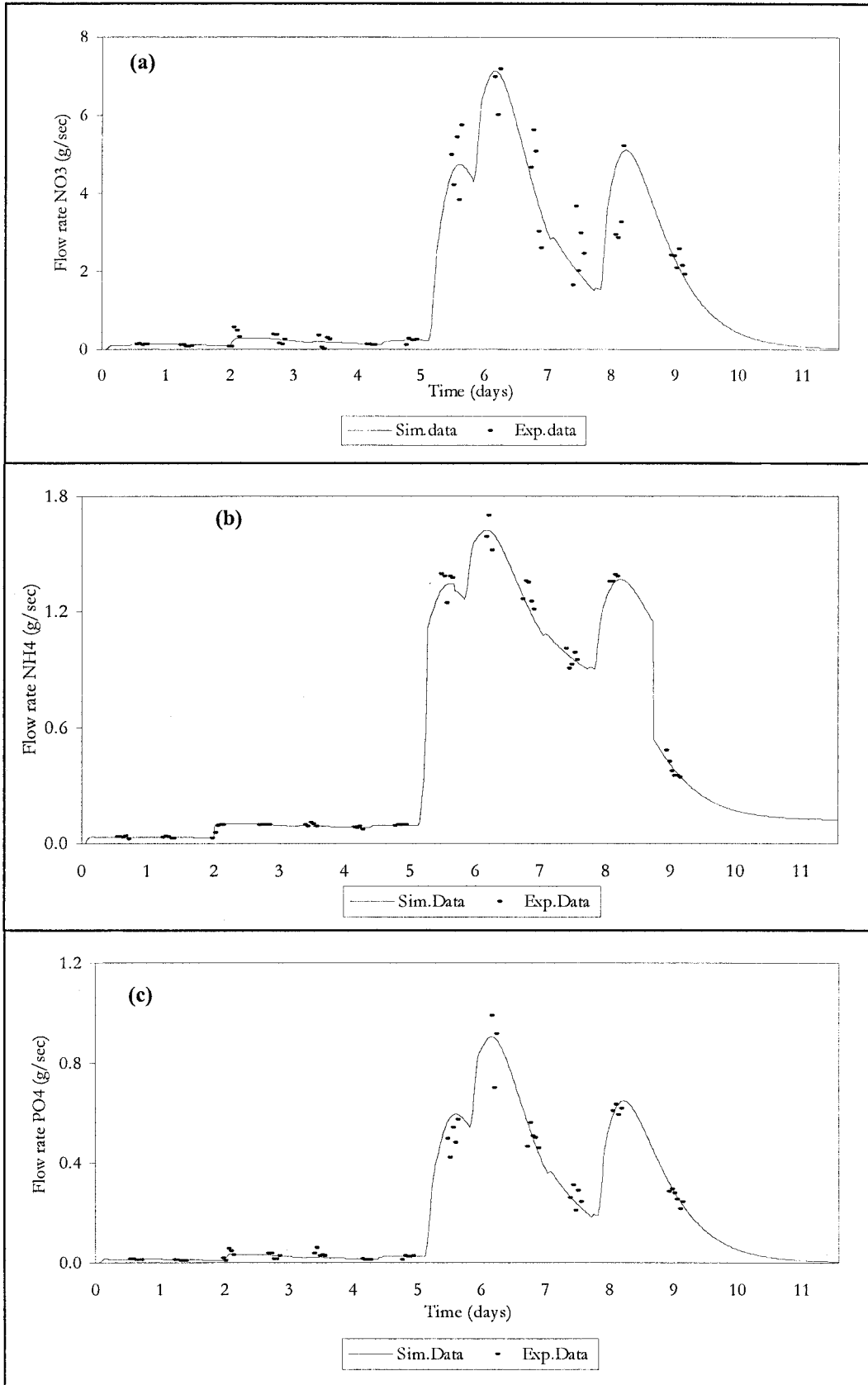
Table 6.   Results of two-sided Kolmogorov-Smirnov goodness-of-fit test between experimental and simulated[a] flow rates of dissolved-phase nitrate, ammonia, and phosphate for 12 storm events or storm periods

Date (m/d/y)	*Nitrate*			*Ammonia*			*Phosphate*		
	Total NO$_3$ observed (kg)	Total NO$_3$ simulated (kg)	K-S test values	Total NH$_4$ observed (kg)	Total NH$_4$ simulated (kg)	K-S test values	Total PO$_4$ observed (kg)	Total PO$_4$ simulated (kg)	K-S test values
9/2/1996	35.1	29.3	0.433	13.2	12.5	0.309[b]	9.1	7.5	0.339[b]
26/2/1996	12.2	10.4	0.417[b]	6.6	5.1	0.443[b]	2.5	1.2	0.376[b]
13/3/1996	13.4	11.5	0.381[b]	5.7	4.5	0.389[b]	2.2	1.3	0.314[b]
5/4/1996	73.3	68.7	0.214[b]	11.1	12.3	0.331[b]	5.4	5.5	0.222[b]
15/4/1996	191	193	0.296[b]	29.2	33.4	0.283[b]	23.2	21.5	0.268[b]
25/11/1996–3/12/1996	1837	1822	0.141[b]	331	339	0.138[b]	197	194	0.122[b]
4/3/1997	65.1	63.3	0.237[b]	12.1	11.4	0.219[b]	9.1	8.4	0.259[b]
2/4/1997	158	155	0.315[b]	37.3	25.2	0.463	25.2	18.1	0.476
10/12/97	16.9	12.1	0.481	5.5	4.7	0.259[b]	2.5	1.8	0.304[b]
22/12/97	58.5	55.3	0.194[b]	10.2	9.1	0.227[b]	5.3	4.5	0.197[b]
3/2/98	81.5	83.7	0.255[b]	19.7	17.3	0.235[b]	8.2	9.1	0.254[b]
10/3/98	100	102	0.214[b]	23.2	25.6	0.158[b]	12.1	13.7	0.192[b]

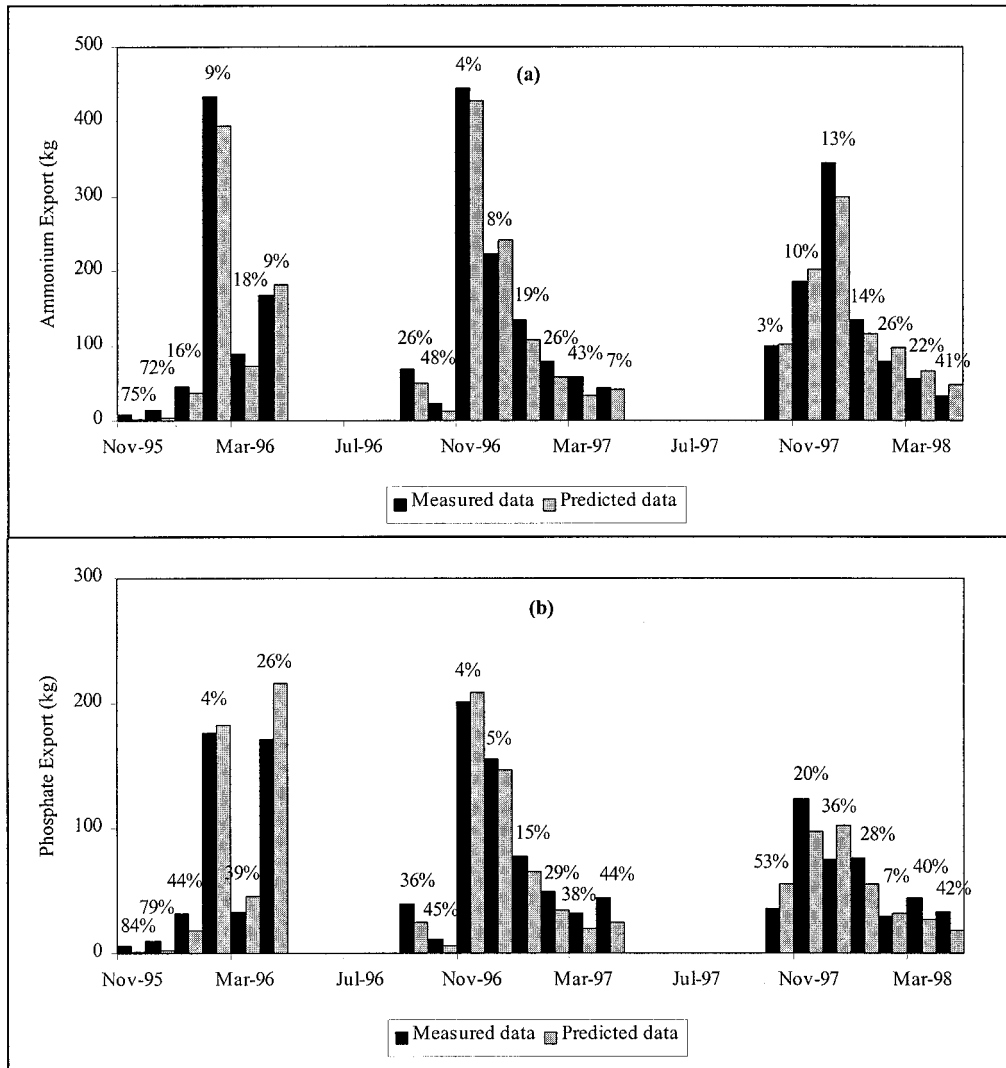[a]Simulated data based on the use of the mass response functions.

[b]Simulated and experimental data not significantly different at the 0.05 level.

the pathway of erosion could be considerable from the maquis areas, with a total amount of 3.08 kg N/km^2/yr and 0.54 kg P/km^2/yr for ammonium and phosphate, respectively. These results were in good agreement with experimental data based on edge-of-field losses (Arhonditsis 1998). Significant quantities of nutrients have also been exported from cultivated olive groves. These discharges can be attributed mostly to the accumulation of inorganic nutrients and organic matter on the topsoil layers due to fertilizer applications and excrement from grazing animals. Soil eroded and delivered from these zones contains a higher percentage of finer and less dense materials (i.e., clay particles or organic residues) accompanied by higher nutrient concentrations than the parent soil due to their greater adsorption capacity. Furthermore, the corresponding values from the abandoned olive groves were less than 0.62 kg N/km^2/yr and 0.24 kg N/km^2/yr, revealing their resistance to these mechanisms of degradation. The reliability of the model in partitioning the total solid-phase nutrient exports and assessing the contribution of the various land-cover categories indicates that it is a useful methodological tool for evaluating alternative management schemes and control practices in order to diminish nonpoint fluxes into surface receiving waters. Additional knowledge about the dynamics of this terrestrial ecosystem will be gained by taking into account wind erosion, a great problem in many regions of the world, which is not modeled by USLE (Beinhauer and Kruse 1994).

Summary and Conclusions

Three well-known models—the runoff curve number equation, the universal soil loss equation and the mass response functions—were calibrated and tested for assessing nonpoint pollution in a typical terrestrial ecosystem in Greece. The relatively good agreement between simulated and experimental data supports the view that they can be proposed as effective estimators for identifying the approximate magnitudes of nonpoint fluxes of nutrients in agricultural runoff and evaluating the likely changes in loading associated with alternative management practices. Furthermore, the study provides several modifications of the general mathematical formulations and experimental values of the model parameters that should be considered essential for literature reviews and further application of these methodologies in similar watersheds within the Mediterranean region.

The main shortcoming of these models involves the simulation of rainfall–runoff events after the extended periods of dryness that frequently characterize the Mediterranean region. Significant inaccuracies were observed between computed and measured values, indicating that basin responses under such extreme conditions are too complex and chaotic to be amenable to conventional process modeling (Nikolaidis and others 1998). However, possible extrapolation of these methods could be accomplished by redefining the empirical equations and regression models for the specific combinations of soil hydrologic groups, land covers, and

Figure 7. Measured versus predicted cumulative monthly exports of solid-phase (**a**) ammonium and (**b**) phosphate from Gera's watershed. The simulated data are based on the use of the Universal Soil Loss Equation. The experimental data result from extrapolation of field measurements on unit plots (Arhonditsis and others 2000b). As a deviation measure between experimental and simulated data was used, the absolute percent error (APE = $100 \times \Pi$ observed value $-$ simulated value Π/observed value).

management under such extreme hydrologic conditions. This effort requires experimental data extracted at broader frameworks and testing of the results at various locations in the Mediterranean area. Moreover, the organization of such an experimental network would also support the stages of sensitivity analysis and validation that so far are totally unexplored, since the present study emphasized only long-term (three-year) model calibration. In this particular case, given the nature of the present models, the basic goal of the sensitivity analysis would be the determination of objective ranges and confidence intervals for all crucial model parameters, whereas validation will test the mod-

els' performance against independent data sets (i.e., nonpoint discharges under different sequences of meteorological events, geomorphological characteristics of the watershed, and agricultural practices that can be encountered in the Mediterranean region). Both sensitivity analysis and validation are essential processes for establishing the reliability of the models (Oreskes and others 1994, Wallach and Genard 1998, Cipra 2000), and their exploration constitutes an aim for on-going studies.

The perspective of decreasing the study time scale of erosion processes was purposely not addressed at this paper, since it was deemed that the present framework

is not adequate for such a complicated goal. Many factors and processes influence the overall process from its sources to the watershed outlet, including re-deposition of sediment in surface water storage, trapping of sediment by vegetation and plant residues, local scour or redeposition in rills and channels, adsorption–desorption mechanisms and decomposition–decay processes to which pollutants are subjected within the run-off (Jolankai 1983). Consequently, extensive water sampling networks and additional analytical approaches (i.e., tracers) should be adopted for supporting more sophisticated modeling efforts, where special emphasis would be given in the description of all the previously mentioned reaction and transformation processes (Peterson and others 2001). This reconsideration of the present experimentation and the development of more refined frameworks seem to be essential for more realistic reproductions of nutrient dynamics in terrestrial ecosystems and more accurate predictions of event-based responses of soil erosion.

Literature Cited

Albertson, M. L., and D. B. Simons. 1964. Fluid mechanics. Chapter 7 *in V. T. Chow (ed.)*, Handbook of applied hydrology. McGraw-Hill, New York.

Alexander, R. B., R. A. Smith, and G. E. Schwarz. 2000. Effect of channel size on the delivery of nitrogen to the Gulf of Mexico. *Nature* 403:758–761.

Arhonditsis, G. 1998. Quantitative assessment of the effects of non-point sources to coastal marine eutrophication. PhD thesis (in Greek, with English abstract), Department of Environmental Studies, University of the Aegean, Mytilene, Greece.

Arhonditsis, G., G. Tsirtsis, G. Angelidis, and M. Karydis. 2000a. Quantification of the effects of non-point nutrient sources to coastal marine eutrophication: Applications to a semi-enclosed gulf in the Mediterranean Sea. *Ecological Modelling* 129(2–3):209–227.

Arhonditsis, G., C. Giourga, and A. Loumou. 2000b. Ecological patterns and comparative nutrient dynamics of natural and agricultural Mediterranean-type ecosystems. *Environmental Management*, 26(5):527–537.

Bagarello, V., and F. D'Asaro. 1994. Estimating single storm erosion index. *Transactions of the American Society of Agricultural Engineering* 37(3):785–791.

Bai, M., J. C. Roegiers, and H. I. Inyang. 1996. Contaminant transport in non-isothermal fractured porous media. *Journal of Environmental Engineering* 122,(5):416–423.

Basnyat, P., L. D. Teeter, K. M. Flynn, and B. G. Lockaby. 1999. Relationships between landscape characteristics and non-point source pollution inputs to coastal estuaries. *Environmental Management* 23:539–549.

Beinhauer, R., and A. Kruse. 1994. Soil erosivity by wind in moderate climates. *Ecological Modelling* 75/76:279–287.

Bendoricchio, G., and A. Rinaldo. 1986. Field scale simulation of nutrient losses. Pages 277–293 in F. Zingales and A. Giorgini (eds.), Agricultural non-point source pollution, model selection and application. Elsevier Scientific Publishing, Amsterdam.

Borah, D. K. 1989. Runoff simulation model for small watersheds. *Transactions of the American Society of Agricultural Engineering* 32(3):881–886.

Bouraoui, F., and T. A. Dillaha. 1996. Answers-2000: Runoff and sediment transport model. *Journal of Environmental Engineering* 122(6):493–502.

Chow, V. T. 1964. Runoff. Section 14 *in* V. T. Chow (ed.), Handbook of applied hydrology. McGraw-Hill, New York.

Chow, V. T., D. R. Maidment, and L. W. Mays. 1988. Applied hydrology. McGraw-Hill New York.

Cipra, B. 2000. Revealing uncertainties in computer models. *Science* 287:960–961.

Crubb, P. J., and A. J. M. Hopkins. 1986. Pages 21–38 *in* B. Dell, A. J. M. Hopkins, and B. B. Lamont (eds.), Resilience in Mediterranean-type ecosystems. Kluwer Academic Publishers, Boston.

Culley, J. L. B., and E. F. Bolten. 1983. Suspended solids and phosphorus loads from clay soil: A watershed study. *Journal of Environmental Quality* 12:498–503.

Deaton, M. L., and J. J. Winebrake. 1999. Dynamic modelling of environmental systems. Springer-Verlag, New York.

Dorioz, J. M., E. Pilleboue, and A. Ferhi. 1989. Phosphorus dynamics in watersheds: Role of trapping processes in sediments. *Water Resources Research* 23:147–158.

Draper, N. R., and H. Smith. 1981. Applied regression analysis. John Wiley & Sons, New York.

Ekholm, P., K. Kallio, E. Turtola, S. Rekolainen, and M. Puustinen. 1999. Simulation of dissolved phosphorus from cropped and grassed clayey soils in southern Finland. *Agriculture, Ecosystems & Environment* 72(3):271–283.

Golfinopoulos, S. K., N. K. Xilourgidis, M. N. Kostopoulou, and T. D. Lekkas. 1998. Use of a multiple regression model for predicting trihalomethane formation. *Water Research*, 9, 2821–2829.

Haith, D. A., and L. J. Tubbs. 1981. Watershed loading functions for nonpoint sources. *Journal of the Environmental Engineering Division*, 107(EE1):121–137.

Hartigan, J. P., T. F. Quasebarth, and E. Southerland. 1983. Calibration of NPS model loading factors. *Journal of Environmental Engineering*, 109(6):1259–1272.

Hatzopoulos, J. N., C. Giourga, S. Koukoulas, and N. Margaris. 1992. Land cover classification of olive trees in Greek islands using Landsat-TM images. Pages 201–207 in Proceedings of the ASPRS at the International Conference in Washington DC, 2–7 August 1992.

Hauser, V. L., and O. R. Jones. 1991. Runoff curve numbers for the southern High Plains. *Transactions of the American Society of Agricultural Engineering* 34(1):142–148.

Hawkins, R. H. 1978. Runoff curve numbers with varying site moisture. *Journal of the Irrigation and Drainage Division* 104(IR4):389–398.

Huber, A., M. Bach, and H. G. Frede. 2000. Pollution of surface waters with pesticides in Germany: Modeling non-

point source inputs. *Agriculture, Ecosystems & Environment* 80(3):191–204.

Jolankai, G. 1983. Modelling of non-point source pollution. Pages 283–385 *in* S. E. Jorgensen (ed.), Application of ecological modelling in environmental management. Part A. Elsevier Scientific Publishing, Amsterdam.

Kitsiou, D., and M. Karydis. 1998. Development of categorical mapping for quantitative assessment of eutrophication. *Journal of Coastal Conservation* 4:35–44.

Marchetti, R., and N. Verna. 1992. Quantification of the phosphorus and nitrogen loads in the minor rivers of the Emilia-Romagna coast (Italy). A methodological study on the use of theoretical coefficients in calculating the loads. Pages 315–335 *in* R. A. Vollenweider, R. Marchetti and R. Viviani (eds.), Marine Coastal Eutrophication, Elsevier Science Publications, Amsterdam.

Moore, I. D., and J. P Wilson. 1992. Length-slope factors for the revised universal soil loss equation: Simplified method of estimation. *Journal of Soil and Water Conservation* 47(5): 422–428.

Moreno, J. M., and W. C. Oechel. 1995. Global change and Mediterranean-type ecosystems. Springer-Verlag, New York.

Nikolaidis, N. P., H. Heng, R. Semagin, and J. C. Clausen. 1998. Non-linear response of a mixed land use watershed to nitrogen loading. *Agriculture, Ecosystems & Environment* 67(2–3):251–265.

Novotny, V., and G. Chesters. 1981. Handbook of nonpoint pollution: Sources and management, Van Nostrand Reinhold, New York.

Novotny, V., H. Tran, G. V. Sinsiman, and G. Chesters. 1978. Mathematical modeling of land runoff contaminated by phosphorus. *Journal of Water Pollution Control Federation* 1:101–112.

Oreskes, N., K. Shrader-Frechette, and K. Belitz. 1994. Verification, validation and confirmation of numerical models in the earth sciences. *Science*, 263:641–646.

Paerl, H. W. 1997. Coastal eutrophication and harmful algal blooms: Importance of atmospheric deposition and groundwater as 'new' nitrogen and other nutrient sources. *Limnology and Oceanography*, 42(5, part 2):1137–1153.

Peterson, B. J., W. M. Wollheim, P. J. Mulholland, J. R. Webster, J. L. Meyer, J. L. Tank, E. Marti, W. B. Bowden, H. M. Valett, A. E. Hersley, W. H. McDowell, W. K. Dodds, S. K. Hamilton, S. Gregory, and D. D. Morrall. 2001. Control of nitrogen export from watersheds by headwater streams. *Science* 292:86–90.

Renard, K. G., and V. A. Ferreira. 1993. RUSLE model description and database sensitivity. *Journal of Environmental Quality* 22:458–466.

Renard, K. G., G. R. Foster, D. C. Yoder, and D. K. McCool. 1994. RUSLE revisited: Status, questions, answers and the future. *Journal of Soil Water Conservation* 49(3):213–220.

Rinaldo, A., and A. Marani. 1987. Basin scale model of solute transport. *Water Resources Research*, 23(11):2107–2118.

Rosso, R. 1984. Nash model relation to Horton order ratios. *Water Resources Research* 20(7):914–920.

Scholefield, D., and A. C. Stone. 1995. Nutrient losses in runoff water following application of different fertilisers to grassland cut for silage. *Agriculture, Ecosystems & Environment* 55(3):181–191.

Sheridan, J. M., R. Lowrance, and D. D. Bosch. 1999. Managements effects on runoff and sediment transport in riparian forest buffers. *Transactions, American Society of Agricultural Engineers* 42:55–64.

Smith, L. M., and D. M. Patrick. 1991. Erosion, sedimentation and fluvial systems. *Geological Society of America, Centennial Special Volume* 3:169–181.

Summers, R. N., D. Van Gool, N. R. Guise, G. J. Heady, and T. Allen. 1999. The phosphorus content in the run-off from the coastal catchment of the Peen Inlet and Harvey Estuary and its associations with land characteristics. *Agriculture, Ecosystems & Environment* 73(3):271–279.

Vieux, B. E., and S. Needham. 1993. Non-point pollution model sensitivity to grid-cell size. *Journal of Water Resources Planning and Management* 119(2):141–157.

Vounatsou, P., and M. Karydis. 1991. Environmental characteristics in oligotrophic waters: Data evaluation and statistical limitations in water quality studies. *Environmental Monitoring and Assessment* 18:211–220.

Wallach, D., and M. Genard. 1998. Effect of uncertainty in input and parameter values on model prediction error. *Ecological Modelling* 105:337–345.

Watson, D. F., and G. M. Philip. 1985. A refinement of inverse distance weighted interpolation. *Geo-Processing* 2:315–327.

Yoder, D., and J. Lown. 1995. The future of RUSLE: Inside the new revised universal soil loss equation. *Journal of Soil Water Conservation* 50(5):484–489.

Zar, J. H. 1984. Biostatistical analysis, 2nd ed., Prentice-Hall, Englewood Cliffs, New Jersey.

Zingales, F., A. Marani, A. Rinaldo, and G. Bendoricchio. 1984. A conceptual model of unit-mass response function for non-point source pollutant runoff. *Ecological Modelling* 26:285–311.